Published in final edited form as:
J Mol Cell Cardiol. 2013 November ; 64: . doi:10.1016/j.yjmcc.2013.09.001.

Developmental Changes in Expression and Biophysics of Ion Channels in the Canine Ventricle

Jonathan M Cordeiro, PhD[*], **Brian K Panama, PhD**, **Robert Goodrow, BS**, **Andrew C Zygmunt, PhD**, **Casey White, BS**, **Jacqueline A Treat, BS**, **Tanya Zeina, BS**, **Vladislav V Nesterenko, PhD**, **José M Di Diego, MD**, **Alexander Burashnikov, PhD**, and **Charles Antzelevitch, PhD**[*]
Department of Experimental Cardiology Masonic Medical Research Laboratory 2150 Bleecker St. Utica, NY 13501 U.S.A.

Abstract

Background—Developmental changes in the electrical characteristics of the ventricular myocardium are not well defined. This study examines the contribution of inwardly rectifying K^+ current (I_{K1}), transient outward K^+ current (I_{to}), delayed rectifier K^+ currents (I_{Kr} and I_{Ks}) and sodium channel current (I_{Na}) to repolarization in the canine neonate myocardium.

Methods—Single myocytes isolated from the left ventricle of 2-3 week old canine neonate hearts were studied using patch-clamp techniques.

Results—Neonate cells were ~6-fold smaller than those of adults (28.8±8.8 vs. 176±6.7 pF). I_{K1} was larger in neonate myocytes and displayed a substantial inward component and an outward component with negative slope conductance, peaking at −60 mV (4.13 pA/pF). I_{Kr} tail currents (at −40 mV), were small (<20 pA). I_{Ks} could not be detected, even after exposure to isoproterenol (100 nM). I_{to} was also absent in the neonate, consistent with the absence of a phase 1 in the action potential. Peak I_{Na}, late I_{Na} and I_{Ca} were smaller in the neonate compared with adult. *KCND3, KCNIP2* and *KCNQ1* mRNA expression was half, while *KCNH2* was equal and *KCNJ2* was greater in the neonate when compared with adults.

Conclusions—Two major repolarizing K^+ currents (I_{Ks} and I_{to}) present in adult ventricular cells are absent in the 2 week old neonate. Peak and late I_{Na} are significantly smaller in the neonate. Our results suggest that the absence of these two currents in the neonate heart may increase the susceptibility to arrhythmias under certain long QT conditions.

Keywords

K^+ Current; Ventricular arrhythmias; Sudden Death; Developmental Electrophysiology

INTRODUCTION

It is well established that prolongation of the QT interval can increase the risk for developing cardiac arrhythmias. In the neonate heart, prolongation of the QT interval may be due to defects in cardiac ion channels which may be responsible for some reported cases of sudden infant death syndrome (SIDS) [1]. Approximately 95% of all SIDS cases occur

[*]Addresses for correspondence: Jonathan M Cordeiro, Ph.D. Masonic Medical Research Laboratory 2150 Bleecker Street Utica, NY, USA 13501-1787 Phone: (315) 735-2217, ext. 132 FAX: (315) 735-5648 jcordeiro@mmrl.edu or Charles Antzelevitch, Ph.D. Masonic Medical Research Laboratory 2150 Bleecker Street Utica, NY, USA 13501-1787 Phone: (315) 735-2217, ext. 117 FAX: (315) 735-5648 ca@mmrl.edu.

Conflicts of interest/Disclosures: There are no conflicts of interest to disclose.

before the age of 6 months. Recent studies suggest that approximately 1 out of 5 SIDS case may be due ion channel variations [2]. These ion channel defects would be expected to reduce the repolarization reserve of the ventricular myocardium, leading to the development of Torsade de Pointes (TdP) arrhythmias. The extent to which the neonatal canine and human heart is compromised and made vulnerable by mutations and drugs that reduce sodium and/or potassium channel currents is not well understood, because the ionic basis for repolarization in neonate cells are not well defined.

In the adult mammalian heart, marked differences in the shape and duration of the cardiac action potential have been well described in different regions of ventricle [3-5]. These differences are due to differences in a number of time- and voltage-dependent K^+ currents which control repolarization. In adult canine heart at least four K^+ currents play important roles in regulating the cardiac action potential duration: an inwardly rectifying K^+ current, I_{K1}; a Ca^{2+}-independent transient outward K^+ current, I_{to}; and rapid and slow components of the delayed rectifier K^+ currents, I_{Kr} and I_{Ks} [6,7].

In contrast, the neonatal heart exhibits prominent differences in action potential waveform compared to the adult heart. For example, in neonatal ventricular tissue isolated from dog [8,9] and rat [10] the very rapid phase 1 (normally present in adult tissue) is small or absent, suggesting that I_{to}, is absent. In addition, other experimental studies demonstrated that class III anti-arrhythmic agents produce a greater prolongation on action potential duration in the neonatal heart,[11] suggesting that the rapid and slow delayed rectifier currents are reduced in the young heart. These results suggest that the underlying ionic currents are different at different stages of development. However, the complement of K^+ currents is not well understood at the early stages of development in the canine heart.

The present study was designed to examine the contribution of sodium channel current (I_{Na}), I_{Ca}, I_{K1}, I_{to} , I_{Kr} and I_{Ks} in the 2 week old canine neonate ventricular myocardium. Our data indicate that two of the major repolarizing K^+ currents (I_{Ks} and I_{to}) present in adult ventricular cells are absent in 2 week old neonate ventricular cells. In addition, both peak and late I_{Na} are also reduced in the neonate. Since I_{Ks} is absent in the neonate heart, repolarization is mainly dependent on I_{Kr}. Preliminary results have been presented in abstract form [12,13].

METHODS

Isolation of Neonate Cells

Myocytes were prepared from 2 week old canine hearts using techniques previously described with minor modifications [14]. Briefly, male and female mongrel dogs were anesthetized with sodium pentobarbital (35 mg/kg i.v.), their hearts were rapidly removed and placed in nominally Ca^{2+}-free Tyrode's solution. The heart was then cannulated through the aorta and perfused with nominally Ca^{2+}-free Tyrode's solution containing 0.1% BSA for about 5 minutes. The heart was then subjected to enzymatic digestion with the nominally Ca^{2+}-free solution supplemented with 0.5 mg/ml collagenase (Type II, Worthington) and 1 mg/ml BSA for 7-9 minutes. After perfusion, the left ventricle was removed, minced and incubated in fresh buffer containing 0.5 mg/ml collagenase, 1 mg/ml BSA and agitated. The supernatant was filtered, centrifuged and the pellet containing the myocytes was stored in KB solution at room temperature. All animal procedures were in accordance with previously established guidelines (NRC publication, Guide for care and use of laboratory animals. Eighth Edition. 2011).

Solutions

All solutions were made with Milli-Q grade water. Nominally Ca^{2+}-free buffer had the following composition (mM): NaCl 129, KCl 5.4, $MgSO_4$ 2.0, NaH_2PO_4 0.9, glucose 5.5, $NaHCO_3$ 20. This solution was bubbled with 95% O_2/5% CO_2. The modified KB storage solution [15] had the following composition (mM): potassium glutamate 100, potassium aspartate 10, KCl 25, KH_2PO_4 10, $MgSO_4$ 2, taurine 20, creatine 5, EGTA 0.5, glucose 20, HEPES 5, BSA 0.2%, pH adjusted to 7.2 with KOH. Myocytes were superfused with Tyrode's solution of the following composition (mM): NaCl 140, KCl 4, $MgCl_2$ 1.0, $CaCl_2$ 2.0, HEPES 10, and glucose 10. pH was adjusted to 7.4 with NaOH.

Action Potential and Voltage Clamp Recordings of K^+ Currents

Voltage and current clamp recordings were made using both whole cell and amphotericin perforated patch techniques [7,16]. Patch pipettes were fabricated from glass capillaries (1.5 mm O.D., Fisher Scientific, Pittsburg, PA). Patch pipettes were pulled from glass capillaries (1.5 mm o.d. and 1.1 mm i.d.) on a Model PP-830 vertical puller (Narashige Instruments, Japan) and filled with pipette solution of the following composition (mM): potassium aspartate 120, KCl 10, HEPES 10.0, $MgCl_2$ 1.0, EGTA 5.0, NaCl 10. pH was adjusted to 7.2 with KOH. In some experiments, amphotericin B (240 μg/ml) was included in the pipette solution. The pipette resistance ranged from 2-4 MΩ when filled with the internal solution. Action potentials were elicited using a 3 ms current pulse at 120% threshold amplitude and cells were paced at a cycle length of 1 Hz. Current and voltage signals were recorded using a MultiClamp 700A amplifier (Molecular Devices Inc., Foster City, CA) and series resistance errors were electronically compensated by 70-80%. All signals were acquired at 5-50 kHz (Digidata 1322, Molecular Devices) and analyzed with pClamp 9 software (Molecular Devices). All K^+ current experiments were performed at 36° C.

Voltage Clamp Recordings of Peak I_{Na}

Early sodium current, I_{Na}, was measured as previously described with minor modifications [17,18]. Patch pipettes were pulled from glass capillaries and the electrode resistance was 0.9-2.0 MΩ when filled with the internal solution (see below). The membrane was ruptured by applying negative pressure and series resistance compensated by 70-80%. Whole cell current data was acquired at 20-50 kHz and filtered at 5 kHz. Currents were normalized to cell capacitance.

External solution contained (in mM): Choline Cl 120, NaCl 10, Na^+ acetate 2.8, $CaCl_2$ 0.5, KCl 4, $MgCl_2$ 1.5, $CoCl_2$ 1, glucose 10, HEPES 10, NaOH 5, $BaCl_2$ 0.1, pH adjusted to 7.4 with NaOH/HCl. The pipette solution contained (mM): NaCl 15, CsF 120, $MgCl_2$ 1, KCl 5, HEPES 10, Na_2ATP 4, EGTA 10, pH adjusted to 7.2 with CsOH. Peak sodium current was dramatically reduced in the low extracellular sodium to ensure adequate voltage control, as gauged by the slope of a Boltzmann fit to the steady state activation curve [19] and peak I_{Na} was recorded at room temperature. When measuring sodium channel kinetics and density the holding potential was −120 mV to recruit all available sodium channels. In addition, recordings of I_{Na} were made at least 5 min after rupture to minimize the effects of time-dependent negative shift of steady-state inactivation that occurs in conventional voltage clamp experiments. Whole cell currents were analyzed using the *Clampfit* analysis program from pClamp 9 (Axon Instruments).

Voltage Clamp Recordings of Late I_{Na}

Late I_{Na} density was a measured in full external Na^+ at 37° C as previously described [20,21]. The external solution contained (in mM): NaCl 140, $CaCl_2$ 2.0, $MgCl_2$ 1, glucose 10, HEPES 10, pH adjusted to 7.4 with NaOH. Pipette solution contained (mM): NaCl 10,

aspartate 130, $MgCl_2$ 1, CsCl 10, HEPES 10, MgATP 5, EGTA 10, pH adjusted to 7.2 with CsOH.

Late I_{Na} density was recorded in cells that were held at −80 mV. To remove steady-state inactivation and recruit all Na^+ channels, a pulse to −120 mV was applied before a 500-ms pulse to −40 mV. The protocol was repeated following rapid application of 10 μM TTX. Late I_{Na}, characterized as the TTX-sensitive difference current, was measured as total charge movement during application of the 500 ms step to −40 mV.

Voltage Clamp Recordings of I_{Ca}

I_{Ca} was recorded as previously described with minor modifications [22]. The external solution contained (in mM): NaCl 140, $CaCl_2$ 2.0, $MgCl_2$ 1, glucose 10, HEPES 10, pH adjusted to 7.4 with NaOH. Pipette solution contained (mM): CsCl 120, $MgCl_2$ 1.0, EGTA 10, MgATP 5, HEPES 10, $CaCl_2$ 5, pH=7.2 with CsOH. Ca^{2+} currents were recorded during a 300 msec step depolarization from a holding potential of −40 mV [23].

Isolated ventricular preparations

Left ventricular tissues from epicardial, midmyocardial and endocardial regions (approximately 1.0 × 0.5 × 0.1 cm) were isolated from hearts removed from anesthetized (sodium pentobarbital, 35 mg/kg) 2 week old mongrel dogs. The preparations consisted of dermatome shavings (Davol Simon Dermatome Power Handle 3293 with cutting head 3295, Cranston, R.I.) obtained from the left ventricular free wall. The tissues were superfused with oxygenated (95% O_2/ 5% CO_2) Tyrode's solution maintained at 36-37°C. The composition of the Tyrode's solution was (in mM): NaCl 129, KCl 4, NaH_2PO_4 0.9, $NaHCO_3$ 20, $CaCl_2$ 1.8, $MgSO_4$ 0.5, and D-glucose 5.5; pH=7.4.

All preparations were studied in the same bath and allowed to equilibrate until the action potentials achieved steady-state (usually 4-5 hours). The tissues were stimulated at basic cycle lengths (BCL) ranging from 300 to 2000 ms using rectangular stimuli (2-5 ms duration, 2-2.5 times diastolic threshold intensity) delivered through thin silver bipolar electrodes. Transmembrane action potentials were recorded from the two tissues simultaneously using glass microelectrodes filled with 2.7 M KCl (10-30 MΩ: DC resistance) connected to a high input-impedance amplification system (World Precision Instruments, New Haven, Conn.). Recordings were started 30 min after the addition of d-sotalol or chromanol 293B. The signals were digitized (model 1401 AD/DA system, Cambridge Electronic Designs [C.E.D.]), analyzed (Spike 2 acquisition and analysis module, C.E.D.).

RNA isolation and quantitative real time PCR

Ventricular tissue was washed in Tyrode's solution and immediately frozen in liquid nitrogen before storage at −80 °C. For RNA isolation, the tissue was disrupted with a mortar and pestle and then homogenized with a sterile syringe and needle (19, 20 and 21 gauges). After homogenization, a RNeasy Fibrosis Tissue kit was used to isolate the RNA (Qiagen). A NanoDrop® spectrophotometer (Thermo Scientific) was used to quantify RNA samples. A 28S/18S rRNA ratio was used to assess RNA integrity on a 1.2% formaldehyde gel.

The Superscript™ III Reverse Transcriptase kit (Invitrogen) approach was used to synthesize cDNA from 1-5 μg of RNA, exactly according to the manufacturer protocol. Both SYBR green® (Applied Biosystems) and TaqMan master mix (Applied Biosystems) systems used.

Primers: *KCNIP2* – Cf02630856_m1 (TaqMan); *KCND3* – Cf02698011_m1 (TaqMan) *KCNH2* – Cf02624781_m1 (TaqMan); *KCNJ2* – Cf03022918_s1 (TaqMan); *KCNQ1* – Fwd: ATTCGGCGCATGCAGTACTT; Rev: TTGATGCGCACCATGAGGTT (SYBR green) 18S – Fwd: CGCCGCTAGAGGTTGAAATTC; Rev: TCCGACTTTCGTTCTTGATTAATG (SYBR green)

A Real-Time thermal cycler PCR System 7000 (Applied Biosystems) was used to amplify the cDNA. All no template control wells were negative in all PCR runs. The mRNA levels were referenced to 18S rRNA. For relative quantification, the ΔΔCt method was used [24].

Drugs

Isoproterenol and d-Sotalol were purchased from Sigma (St. Louis, MO). HMR-1556 and chromanol 293B were generous gifts from Aventis Pharmaceutical (Germany). E-4031 was a generous gift from Eisai Co.

Statistics

Results from pooled data are presented as Mean±SEM. Statistical analysis was performed using an ANOVA test followed by a Student-Newman-Keuls test or a Student t-test, as appropriate, using SigmaStat software. A $p<0.05$ was considered statistically significant.

RESULTS

Developmental Differences in K^+ Currents in Ventricular Myocytes

Action potentials (AP) were recorded from epicardial, endocardial and midmyocardial strips of tissue. Figure 1A shows that AP waveforms recorded from the three left ventricular cell layers are homogeneous in the 2 week old dog. The preparations were stimulated at a cycle length of 2 sec. All three APs lacked the spike and dome configuration typically observed in adult cells and displayed a similar AP duration (APD). The compound chromanol 293B has been reported to inhibit both I_{Ks} and I_{to} in ventricular myocytes [25]. Since neonate APs lacked phase 1 repolarization suggesting absence of I_{to}, we determined the effect of I_{Ks} blockade with chromanol 293B. Application of chromanol 293B (30 μM) did not significantly prolong APD in any of the tissue types. The I_{Kr} blocker d-sotalol (100 μM) prolonged APD to a similar extent in all three cell types, further confirming the homogeneous nature of the ventricle in the 2 week old dog. Table 1 summarizes the effects of chromanol 293B and sotalol on APD_{90} and development of early afterdepolarizations (EADs) in 7-10 day old neonatal tissue.

We next determined the ionic basis for action potential distinctions between cells isolated from adult and 2 week old dogs. Our data confirm that the ventricular myocardium in the 2 week old dog is homogeneous [26] and, therefore, we did not separate myocytes from the three distinct layers (epi-, mid- and endo- layers). Adult ventricular cells were significantly larger and displayed more distinct cross-striations than neonate ventricular cells (Figure 2). Input resistance (R_{in}; measured by applying small hyperpolarizing currents from the resting potential) of the neonatal ventricular cell averaged 419±31 MΩ (n=6) with a mean capacitance (C_m) of 28.8±8.8 pF (n=29). In contrast, adult ventricular cells yielded R_{in} values of 31.8±8.9 MΩ (n=10) and C_m values of 176±6.7 pF (n=17).

Figure 3 shows representative APs (Panel A) and a family of currents (Panel B) recorded from the same neonate and adult ventricular myocyte. In response to hyperpolarizing voltage clamp pulses, the absolute magnitude of I_{K1} was much smaller in neonatal cells than adult myocytes. At more positive potentials, adult, but not neonatal cells, displayed a transient

outward current (I_{to}) consistent with the presence of phase 1 repolarization in adult but not neonatal cells.

We next examined the current properties of I_{K1} in neonate cells. Figure 4 shows the dependence of I_{K1}, measured as a barium sensitive current, on $[K^+]_o$ in a neonatal cell. Figure 4A shows representative I_{K1} currents measured from a neonate cell measured in 4 or 10 mM K^+ in the absence and presence of 100 μM $BaCl_2$, which inhibited the current. I-V relations of the barium-sensitive current are depicted in Figure 4B. Increasing $[K^+]_o$ from 4 to 10 mM led to an increase in the magnitude of I_{K1} and cross-over phenomenon in the neonatal cells, as has been previously demonstrated for adult cells [27-29]. Measurement of I_{K1} in adult M cells (4 mM K^+ external) showed that the density of I_{K1} was smaller in adult than neonate ventricular cells (Figure 4C).

In adult canine ventricular cells, the outward component of I_{K1} is largely responsible for the terminal phase of repolarization of the AP. We evaluated the contribution of I_{K1} to the AP in the neonate using the action potential clamp technique (Figure 5). A previously recorded ventricular action potential from a 2-week neonate served as the template (Figure 5A). Currents measured in response to the AP clamp before and after rapid application of 100 μM $BaCl_2$ are shown in Figure 5B. Subtraction of the $BaCl_2$ trace from the control trace results in the Ba^{2+}-sensitive difference current shown in Figure 5C. Results show that I_{K1} (measured as the Ba^{2+}-sensitive difference current) contributes predominantly to final portion of phase 3 in the neonate, as in the adult. The outward component of I_{K1} contributes 58.9±6.7 pA (n=5) or 2.15±0.18 pA/pF when normalized for cell size. By comparison, the outward component of I_{K1} in adult mid cells contributes 340.8±15.5 pA (n=6) or 1.83±0.08 pA/pF when normalized for cell size. These values are similar to previous reports on I_{K1} in dog [30]

In adult canine ventricular cells, the slowly and rapidly activating delayed rectifier (I_{Ks} and I_{Kr}, respectively) contribute to phase 3 repolarization of the AP. Figure 6A shows voltage clamp recordings of I_{Kr} tail currents recorded from 2 week old neonate. A small but measurable tail current was observed upon repolarization to −40 mV. In several experiments, the identity of the tail current was confirmed by addition of the I_{Kr} specific blocker, E-4031. Application of E-4031 (5 μM) completely abolished the tail current confirming the identity of this current. Figure 6B shows the average I-V relationship for I_{Kr}. Peak I_{Kr} tail current density was observed at approximately +20 mV and averaged 0.45±0.08 pA/pF (n=8), similar to values previously reported for adult canine ventricular cells [31-34].

Using longer test pulses (1000 ms), we attempted to measure I_{Ks} in 2 week old neonatal cells. Figure 7A shows currents recorded from a neonatal cell pretreated with E-4031 (5 μM) to remove contaminating currents due to I_{Kr}. No perceptible I_{Ks} tail current was observed (n=9) under baseline conditions. In contrast, I_{Ks} tail currents were readily measureable in adult ventricular mid cell with a peak current density of 0.39±0.04 pA/pF (n=6) at +40 mV (Figure 7D). In neonate cells, isoproterenol (100 nM) was introduced to enhance I_{Ks} (Figure 7B) but failed to do so (n=5), further confirming that I_{Ks} is not present at this stage of development. Application of isoproterenol did cause a substantial increase in the magnitude of I_{Ca} confirming the presence of ß-adrenergic receptors in 2 week old neonate ventricle.

To examine the molecular basis for the differences potassium channel currents between neonatal and adult hearts, we measured gene expression of *KCND3, KCNIP2, KCNQ1, KCNH2* and *KCNJ2*. Neonatal ventricular tissue had more than 2-fold less *KCND3, KCNIP2* and *KCNQ1* expression compared with adult, while *KCNH2* expression was not

different (Figure 7C). On the other hand, adult ventricle had less *KCNJ2* when compared with that of neonate.

Developmental Changes in Inward Currents I_{Na} and I_{Ca}

The reduced repolarization reserve due to the absence of I_{to} and I_{Ks} would suggest that the neonate heart would be more susceptible to arrhythmias following application of either an I_{Kr} or I_{Ks} blocker (Figure 1). However, in our experiments arrhythmias were rarely observed. These observations suggest that depolarizing currents may also be reduced in the neonate heart. We first compared the density on I_{Na} in neonate versus adult ventricular cells. Peak I_{Na} was measured in low extracellular sodium buffer at room temperature to ensure adequate voltage control. Representative I_{Na} traces recorded from a neonate and adult ventricular Endo cell are shown in Figure 8A-B. Results of the experiments demonstrate that the density of I_{Na} is significantly smaller in neonate ventricular cells (Figure 8C).

Since peak I_{Na} (during the 25 ms test pulse) was reduced in neonate cells, it suggests that the persistent or late current would also be smaller. We next measured late I_{Na} during a 500 ms test pulse. Late I_{Na} recordings were performed in full external Na^+ at 37° C. Currents were measured at −40 mV and late I_{Na} was defined as the TTX-sensitive current (Figures 8D-E). Late I_{Na} was quantified as total charge and was found to be significantly smaller in neonates vs. adult midmyocardial cells (−85.9±12.7 pC vs. −215.1±44.3 pC, respectively $p<0.05$).

We next quantified peak I_{Ca} elicited during application of a 300 ms test pulse. Shown are representative I_{Ca} traces recorded from a neonate (Figure 9A) and adult ventricular (Figure 9B) in response to the voltage clamp protocol (top of figure). Peak I_{Ca} was found to be significantly smaller in neonate ventricular cells compared to adult cells (Figure 9C).

DISCUSSION

The principal finding of the present study is that 2 of the major repolarizing K^+ currents (I_{Ks} and I_{to}) present in adult ventricular cells are absent in 2 week old neonate ventricular cells. Only I_{K1} and I_{Kr} could be observed at this stage of development. The small size of neonatal cells (typically 28 pF) did not appear to hamper our ability to record small currents as we were able detect I_{Kr} under our recording conditions. The absence of I_{Ks} was confirmed by gene expression analysis, which showed that KCNQ1 (the pore forming subunit of the I_{Ks} channel) was minimally expressed at the mRNA level (Figure 7). The reduction in repolarization reserve did not result in increased susceptibility to arrhythmias due to either I_{Kr} or I_{Ks} blockade. Analysis of inward I_{Na} and I_{Ca} also showed these currents were significantly smaller compared to adult cells

Regional differences of I_{K1} density have been reported. The current is large in the ventricle, intermediate in Purkinje cells [7], small in atria [35,36] and virtually absent in pacemaker cells [37]. Whole cell voltage clamp measurement of I_{K1} has demonstrated that changing $[K^+]_o$ results in an increase magnitude of I_{K1} and a cross over effect [28,38]. Our results indicate that these characteristics of I_{K1} are present in cells isolated from the 2 week neonatal heart (Figure 4B). However, when I_{K1} was measured in neonate and adult ventricular cells, we found that the density of this current was greater in neonate cells compared to adults. This was supported by mRNA data showing that *KCNJ2* gene expression, which encodes Kir2.1, is higher in the neonate. By comparison, *KCNJ2* expression is not different between canine embryo and adult hearts [39]. Given that two of the repolarizing currents (I_{to} and I_{Ks}) are absent in neonates, the larger I_{K1} density apparently may compensate for the absence of the I_{Ks}.

Although cell size is very small at this stage of development, our attempts to directly measure I_{Kr} and I_{Ks} in neonate cells yielded unequivocal results. It is unlikely that our inability to record I_{Ks} currents was due to enzyme degradation and myocyte damage during isolation [40] since (i) the action potential exhibited little change in response to I_{Ks} blockade in tissue slices (Figure 1) and (ii) resting potential was stable in these cells.

I_{to} is completely absent in myocytes from 2 weeks (Figure 3). As such, the I_{to} pore forming subunit, *KCND3*, and beta-subunit, *KChIP2*, where lower in the neonate versus adult, which also parallels that of canine embryo and adult [39]. The development of I_{to} with maturity has previously been reported. In the canine myocardium it is believed that I_{to} begins to develop 2 months after birth [8]. The absence of a prominent phase 1 or spike and dome morphology of the epicardial action potential is consistent with the absence of I_{to} (Figure 1), as previously reported in the canine neonate [8]. In the rat myocardium, the appearance of I_{to} occurred at 2 weeks after birth[10]. Furthermore, in the rat the increase in I_{to} appears to be dependent on an increase in serum thyroid hormone [41]. It is unclear when I_{Ks} begins to develop or if it is appearance is triggered by circulating hormones, although previous studies have suggested that the appearance of I_{Ks} is highly variable, appearing between 30-120 days of age in canine neonates [26]. Indeed, *KCNQ1* gene expression was decreased in 2 week old neonatal hearts (Figure 7C).

The absence of two major repolarizing K^+ currents (I_{to} and I_{Ks}) in the neonatal ventricular cells suggest that repolarization reserve may be more labile than in adult ventricular cells. Because I_{Ks} is absent in the neonate heart, phase 3 repolarization depends more critically on I_{Kr}. As a consequence, neonatal cells may be more susceptible to the development of early afterdepolarizations secondary to I_{Kr} or I_{K1} blockade compared to adult ventricular cells [42]. Indeed, the I_{Kr} inhibitor d-sotalol, causes a very significant prolongation of the action potential in neonate cells (Figure 1). However, early afterdepolarizations or other arrhythmias were never observed in any cell layer following application of sotalol (Table 1). These observations suggest that although repolarization is critically dependent on I_{Kr} in the neonate, I_{Kr} blockade produces a homogenous increase in APD, and prevents dispersion of repolarization, a known substrate for arrhythmias. This prolongation, although comparable to that observed in adult M cells, is greater than that observed in adult epicardial or endocardial cells [43]. The lower vulnerability of the neonate heart to I_{Kr} inhibition is likely due to a smaller contribution of late I_{Na} to the action potential. Late I_{Na} inhibition is a well-established antiarrhythmic tactic in acquired long QT syndromes.[44]

In a similar study, Obreztchikova et al. [26] observed a significant and homogeneous prolongation of repolarization in three canine LV tissue types isolated from neonatal dogs (1-19 day old). The incidence of EAD in response to the I_{Kr} blocker, dofetilide, was much smaller in neonates compared to adults. Interestingly, *in situ* dofetilide-induced pro-arrhythmia occurred in 0% of neonate and 40% of adult canine hearts[26]. A lower safety factor (or reduced repolarization reserve [45]) may be attributable to non-linearities in inwardly rectifying K^+ conductance, namely I_{K1} [46] and I_{Kr} [47]. Under our recording conditions (4 mM external K^+), neonatal cells exhibited normal repolarization. However, the dependence of both I_{K1} and I_{Kr} on external K^+ suggests that a reduction in external K^+ would have a profound effect on cardiac repolarization by reducing the magnitude of the 2 repolarizing K^+ currents in neonate hearts.

Although our study focused on ventricular cells, it is unknown whether atrial cells express the same K^+ currents at this stage of development. In adults, the magnitude of I_{K1} is much smaller in atrial tissue versus ventricular tissue [35] suggesting a reduced repolarization reserve in atrial tissue compared to ventricular tissue.

Our results provide insight into the mechanism(s) of repolarization and the underlying ionic currents in canine neonate ventricular cells and demonstrate the major differences in currents between neonate and adult hearts. It is unclear whether the human myocardium exhibits these same differences. If so, human neonatal ventricular myocardium may be more susceptible to the development of arrhythmias following a further inward shift in the balance of current secondary to ion channel mutations, particularly those causing a major gain of function of sodium channel current. It is noteworthy that 1% of cases of sudden infant death syndrome have been attributed to mutations in the sodium channel beta subunits [48].

Acknowledgments

The authors are grateful to Judy Hefferon and Art Iodice for expert technical assistance.

Funding sources: This study was supported by grant HL47678 from NHLBI (CA), NYSTEM grant # C026424 (CA) and the Masons of New York State, Florida, Massachusetts and Connecticut.

References

1. Schwartz PJ, Stramba-Badiale M, Segantini A, Austoni P, Bosi G, Giorgetti R, et al. Prolongation of the QT interval and the sudden infant death syndrome. N Engl J Med. 1998; 338:1709–14. [PubMed: 9624190]
2. Klaver EC, Versluijs GM, Wilders R. Cardiac ion channel mutations in the sudden infant death syndrome. Int J Cardiol. 2011; 152:162–70. [PubMed: 21215473]
3. Sicouri S, Antzelevitch C. A subpopulation of cells with unique electrophysiological properties in the deep subepicardium of the canine ventricle. The M cell. Circ Res. 1991; 68:1729–41.
4. Clark RB, Bouchard RA, Salinas-Stefanon E, Sanchez-Chapula J, Giles WR. Heterogeneity of action potential waveforms and potassium currents in rat ventricle. Cardiovasc Res. 1993; 27:1795–9. [PubMed: 8275526]
5. Fedida D, Giles WR. Regional variations in action potentials and transient outward current in myocytes isolated from rabbit left ventricle. Journal of Physiology (London). 1991; 442:191–209. [PubMed: 1665856]
6. Liu DW, Gintant GA, Antzelevitch C. Ionic bases for electrophysiological distinctions among epicardial, midmyocardial, and endocardial myocytes from the free wall of the canine left ventricle. Circ Res. 1993; 72:671–87. [PubMed: 8431990]
7. Dumaine R, Cordeiro JM. Comparison of K^+ currents in cardiac Purkinje cells isolated from rabbit and dog. J Mol Cell Cardiol. 2007; 42:378–89. [PubMed: 17184792]
8. Jeck CD, Boyden PA. Age-related appearance of outward currents may contribute to developmental differences in ventricular repolarization. Circ Res. 1992; 71:1390–403. [PubMed: 1423935]
9. Pacioretty LM, Gilmour RF Jr. Developmental changes in the transient outward potassium current in canine epicardium. Am J Physiol. 1995; 268:H2513–H2521. [PubMed: 7611502]
10. Shimoni Y, Fiset C, Clark RB, Dixon JE, McKinnon D, Giles WR. Thyroid hormone regulates postnatal expression of transient K^+ channel isoforms in rat ventricle. J Physiol. 1997; 500(Pt 1): 65–73. [PubMed: 9097933]
11. Elizalde A, Barajas H, Navarro-Polanco R, Sanchez-Chapula J. Frequency-dependent effects of 4-aminopyridine and almokalant on action-potential duration of adult and neonatal rabbit ventricular muscle. J Cardiovasc Pharmacol. 1999; 33:352–9. [PubMed: 10069668]
12. Cordeiro JM, Zygmunt AC, Dumaine R, Goodrow RJ, Antzelevitch C. Repolarizing Currents in Canine Neonate Ventricular Myocytes. Pacing and Clinical Electrophysiology. 2003; 26:1086.
13. Panama BK, White C, Cordeiro JM, Zygmunt AC, Goodrow R, Antzelevitch C. Developmental changes in potassium channel expression in the canine heart: implications for sudden infant death caused by arrhythmias. Biophys J. 2013; 104:295a.
14. Cordeiro JM, Malone JE, Di Diego JM, Scornik FS, Aistrup GL, Antzelevitch C, et al. Cellular and subcellular alternans in the canine left ventricle. Am J Physiol Heart Circ Physiol. 2007; 293:H3506–H3516. [PubMed: 17906109]

15. Isenberg G, Klockner U. Calcium tolerant ventricular myocytes prepared by preincubation in a "KB medium". Pflugers Arch. 1982; 395:6–18. [PubMed: 7177773]
16. Calloe K, Soltysinska E, Jespersen T, Lundby A, Antzelevitch C, Olesen SP, et al. Differential effects of the transient outward K^+ current activator NS5806 in the canine left ventricle. J Mol Cell Cardiol. 2010; 48:191–200. [PubMed: 19632239]
17. Cordeiro JM, Mazza M, Goodrow R, Ulahannan N, Antzelevitch C, Di Diego JM. Functionally distinct sodium channels in ventricular epicardial and endocardial cells contribute to a greater sensitivity of the epicardium to electrical depression. Am J Physiol Heart Circ Physiol. 2008; 295:H154–H162. [PubMed: 18456729]
18. Murphy L, Renodin DM, Antzelevitch C, Di Diego JM, Cordeiro JM. Extracellular proton depression of peak and late sodium current in the canine left ventricle. Am J Physiol Heart Circ Physiol. 2011; 301:H936–H944. [PubMed: 21685271]
19. Kaab S, Nuss HB, Chiamvimonvat N, O'Rourke B, Pak PH, Kass DA, et al. Ionic mechanism of action potential prolongation in ventricular myocytes from dogs with pacing-induced heart failure. Circ Res. 1996; 78:262–73. [PubMed: 8575070]
20. Zygmunt AC, Eddlestone GT, Thomas GP, Nesterenko VV, Antzelevitch C. Larger late sodium conductance in M cells contributes to electrical heterogeneity in canine ventricle. Am J Physiol. 2001; 281:H689–H697.
21. Zhou Q, Zygmunt AC, Cordeiro JM, Siso-Nadal F, Miller RE, Buzzard GT, et al. Identification of Ikr kinetics and drug binding in native myocytes. Ann Biomed Eng. 2009; 37:1294–309. [PubMed: 19353268]
22. Calloe K, Goodrow R, Olesen SP, Antzelevitch C, Cordeiro JM. Tissue specific effects of acetylcholine in the canine heart. Am J Physiol Heart Circ Physiol. 2013
23. Cordeiro JM, Greene L, Heilmann C, Antzelevitch D, Antzelevitch C. Transmural heterogeneity of calcium activity and mechanical function in the canine left ventricle. Am J Physiol Heart Circ Physiol. 2004; 286:H1471–H1479. [PubMed: 14670817]
24. Livak KJ, Schmittgen TD. Analysis of relative gene expression data using real-time quantitative PCR and the $2^{-DD}C^T$ Method. Methods. 2001; 25:402–8. [PubMed: 11846609]
25. Sun ZQ, Thomas GP, Antzelevitch C. Chromanol 293B inhibits slowly activating delayed rectifier and transient outward currents in canine left ventricular myocytes. J Cardiovasc Electrophysiol. 2001; 12:472–8. [PubMed: 11332571]
26. Obreztchikova MN, Sosunov EA, Plotnikov A, Anyukhovsky EP, Gainullin RZ, Danilo P, et al. Developmental changes in IKr and IKs contribute to age-related expression of dofetilide effects on repolarization and proarrhythmia. Cardiovasc Res. 2003; 59:339–50. [PubMed: 12909317]
27. Shimoni Y, Clark RB, Giles WR. Role of an Inwardly Rectifying Potassium Current in Rabbit Ventricular Action Potential. Journal of Physiology (London). 1992; 448:709–27. [PubMed: 1593485]
28. Nichols CG, Makhina EN, Pearson WL, Sha Q, Lopatin AN. Inward rectification and implications for cardiac excitability. Circ Res. 1996; 78:1–7. [PubMed: 8603491]
29. Cordeiro JM, Spitzer KW, Giles WR. Repolarizing K^+ currents in rabbit heart Purkinje cells. J Physiol. 1998; 508(Pt 3):811–23. [PubMed: 9518735]
30. Banyasz T, Magyar J, Szentandrassy N, Horvath B, Birinyi P, Szentmiklosi J, et al. Action potential clamp fingerprints of K+ currents in canine cardiomyocytes: their role in ventricular repolarization. Acta Physiol (Oxf). 2007; 190:189–98. [PubMed: 17394574]
31. Liu DW, Antzelevitch C. Characteristics of the delayed rectifier current (I_{Kr} and I_{Ks}) in canine ventricular epicardial, midmyocardial and endocardial myocytes: A weaker I_{Ks} contributes to the longer action potential of the M cell. Circulation Research. 1995; 76:351–65. [PubMed: 7859382]
32. Gintant GA. Characterization and functional consequences of delayed rectifier current transient in ventricular repolarization. Am J Physiol Heart Circ Physiol. 2000; 278:H806–H817. [PubMed: 10710349]
33. Li GR, Lau CP, Ducharme A, Tardif JC, Nattel S. Transmural action potential and ionic current remodeling in ventricles of failing canine hearts. Am J Physiol Heart Circ Physiol. 2002; 283:H1031–H1041. [PubMed: 12181133]

34. Varro A, Balati B, Iost N, Takacs J, Virag L, Lathrop DA, et al. The role of the delayed rectifier component IKs in dog ventricular muscle and Purkinje fibre repolarization. J Physiol (Lond). 2000; 523(Pt 1):67–81. [PubMed: 10675203]
35. Giles WR, Imaizumi Y. Comparison of potassium currents in rabbit atrial and ventricular cells. J Physiol (Lond). 1988; 405:123–45. [PubMed: 2855639]
36. Hume JR, Uehara A. Ionic basis of the different action potential configurations of single guinea-pig atrial and ventricular myocytes. J Physiol (Lond). 1985; 368:525–44. [PubMed: 2416918]
37. Irisawa H, Brown HF, Giles WR. Cardiac pacemaking in the sinoatrial node. Physiol Rev. 1993; 73:197–227. [PubMed: 8380502]
38. Carmeliet E. Induction and removal of inward-going rectification in sheep cardiac Purkinje fibres. J Physiol. 1982; 327:285–308. [PubMed: 6288926]
39. Gonczi M, Birinyi P, Balazs B, Szentandrassy N, Harmati G, Konczei Z, et al. Age-dependent changes in ion channel mRNA expression in canine cardiac tissues. Gen Physiol Biophys. 2012; 31:153–62. [PubMed: 22781818]
40. Salata JJ, Jurkiewicz NK, Jow B, Folander K, Guinosso PJ, Raynor B, et al. Ik of rabbit ventricle is composed of two currents: evidence for Iks. Am J Physiol. 1996; 271:H2477–H2489. Heart Circ. Physiol. 40. [PubMed: 8997308]
41. Wickenden AD, Kaprielian R, Parker TG, Jones OT, Backx PH. Effects of development and thyroid hormone on K^+ currents and K^+ channel gene expression in rat ventricle. J Physiol. 1997; 504(Pt 2):271–86. [PubMed: 9365903]
42. Antzelevitch C. Molecular biology and cellular mechanisms of brugada and long QT syndromes in infants and young children. J Electrocardiol. 2001; 34:177–81. [PubMed: 11781953]
43. Liu DW, Antzelevitch C. Characteristics of the delayed rectifier current (IKr and IKs) in canine ventricular epicardial, midmyocardial, and endocardial myocytes. Circulation Research. 1995; 76:351–65. [PubMed: 7859382]
44. Antzelevitch C, Burashnikov A, Sicouri S, Belardinelli L. Electrophysiological basis for the antiarrhythmic actions of ranolazine. Heart Rhythm. 2011; 8:1281–90. [PubMed: 21421082]
45. Roden DM. Taking the “Idio” out of “Idiosyncratic”: predicting torsades de pointes. Pacing and Clinical Electrophysiology. 1998; 21:1029–34. [PubMed: 9604234]
46. Harvey RD, Ten Eick RE. Characterization of the inward-rectifying potassium current in cat ventricular myocytes. J Gen Physiol. 1988; 91:593–615. [PubMed: 2455768]
47. Spector PS, Curran ME, Zou AR, Keating MT, Sanguinetti MC. Fast inactivation causes rectification of the I_{Kr} channel. J Gen Physiol. 1996; 107:611–9. [PubMed: 8740374]
48. Tan BH, Pundi KN, Van Norstrand DW, Valdivia CR, Tester DJ, Medeiros-Domingo A, et al. Sudden infant death syndrome–associated mutations in the sodium channel beta subunits. Heart Rhythm. 2010; 7:771–8. [PubMed: 20226894]

Highlights

- Peak and late I_{Na} are reduced in ventricular cells during early development.

- The potassium currents, I_{to} and $I_{Ks,}$ were small or absent in ventricular cells during development.

- Proteins subunits responsible for I_{to} and I_{Ks} were expressed at low levels

- Absence of these 2 currents in the neonate may increase susceptibility to arrhythmias under certain long QT conditions.

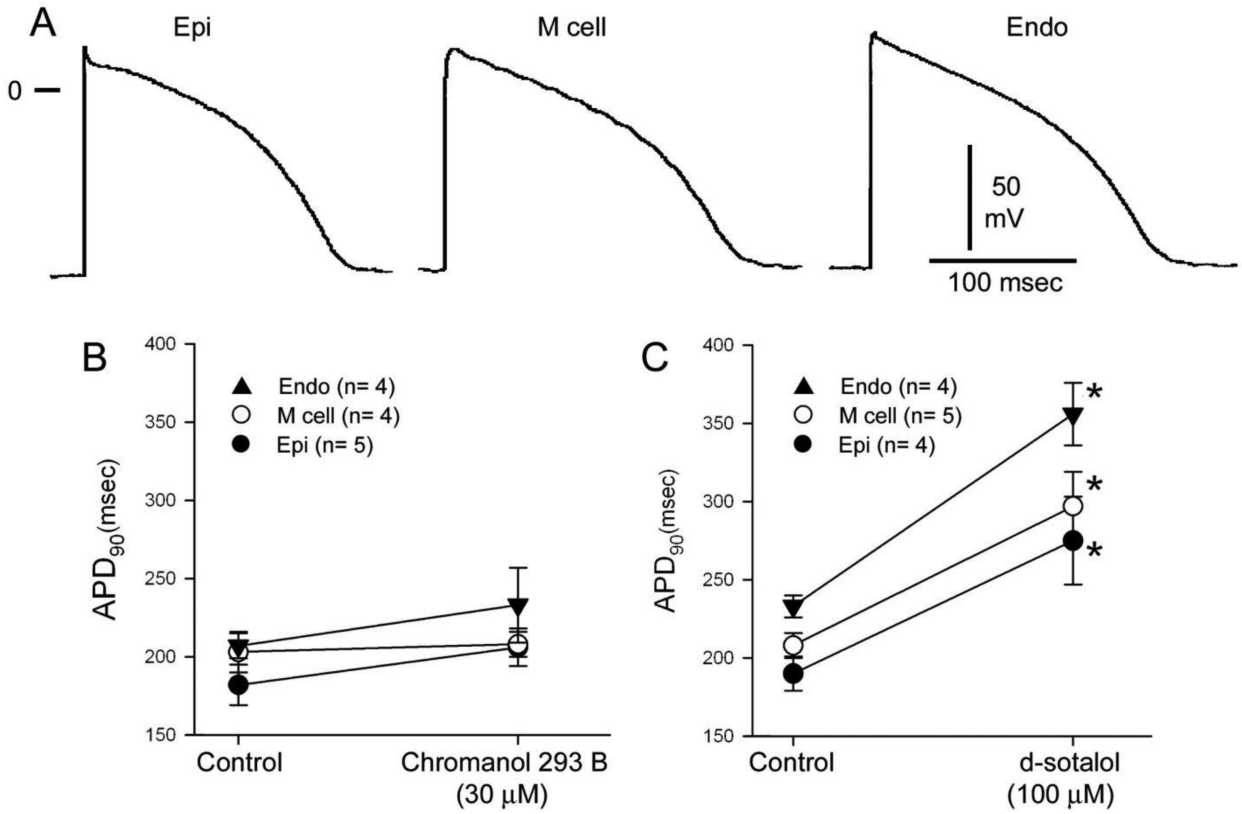

Figure 1.

Panel A: Representative action potentials recorded from ventricular epicardial, midmyocardial and endocardial tissue slices isolated from the 2 week old neonate. Action potentials lack a spike and dome morphology and are of comparable duration. BCL= 2 s. **Panel B:** Application of an I_{Ks} inhibitor (chromanol 293B, 30 μM) failed to alter action potential duration. **Panel C:** Application of an I_{Kr} inhibitor (d-sotalol, 100 μM) produced a very significant homogeneous prolongation of APD in all 3 cell types.

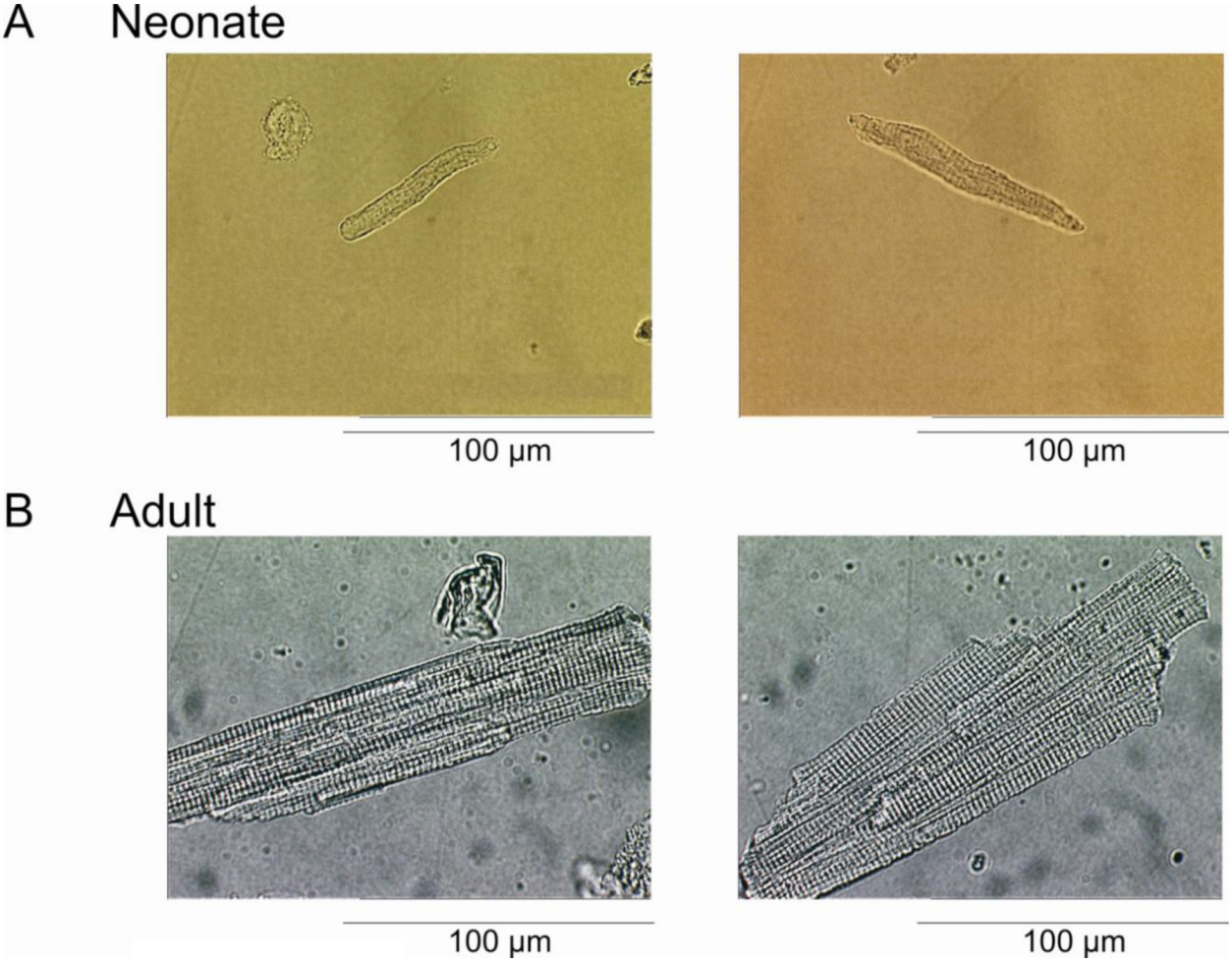

Figure 2.
Photomicrograph of enzymatically isolated canine 2 week-old neonate (**Panel A**) and adult ventricular myocytes (**Panel B**). Neonate cells were typically 6 times smaller, averaging 29±8.8pF.

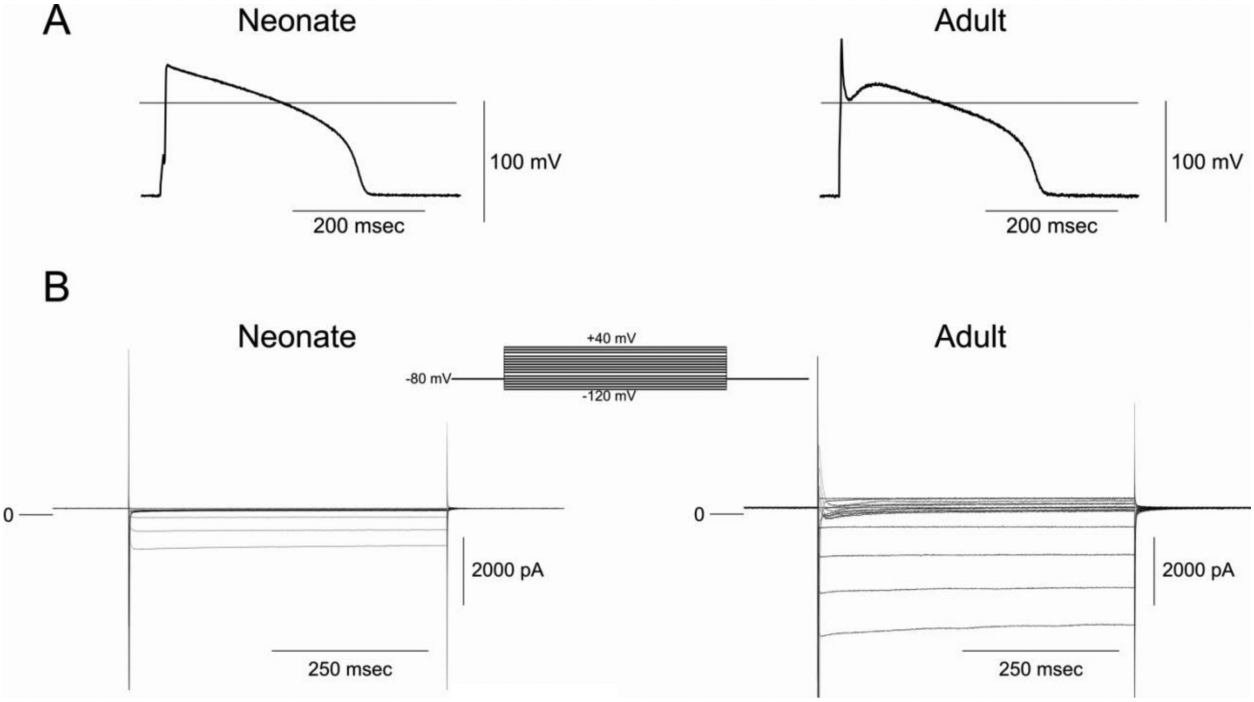

Figure 3.

Panel A: Representative action potentials recorded from a 2 week-old neonate and adult ventricular myocytes. BCL= 2 s. **Panel B:** Comparison of membrane currents recorded from a neonate and adult venticular cell. The myocytes were held at −80 mV and membrane currents were elicited by stepping the voltage to membrane potentials between −110 and +50 mV.

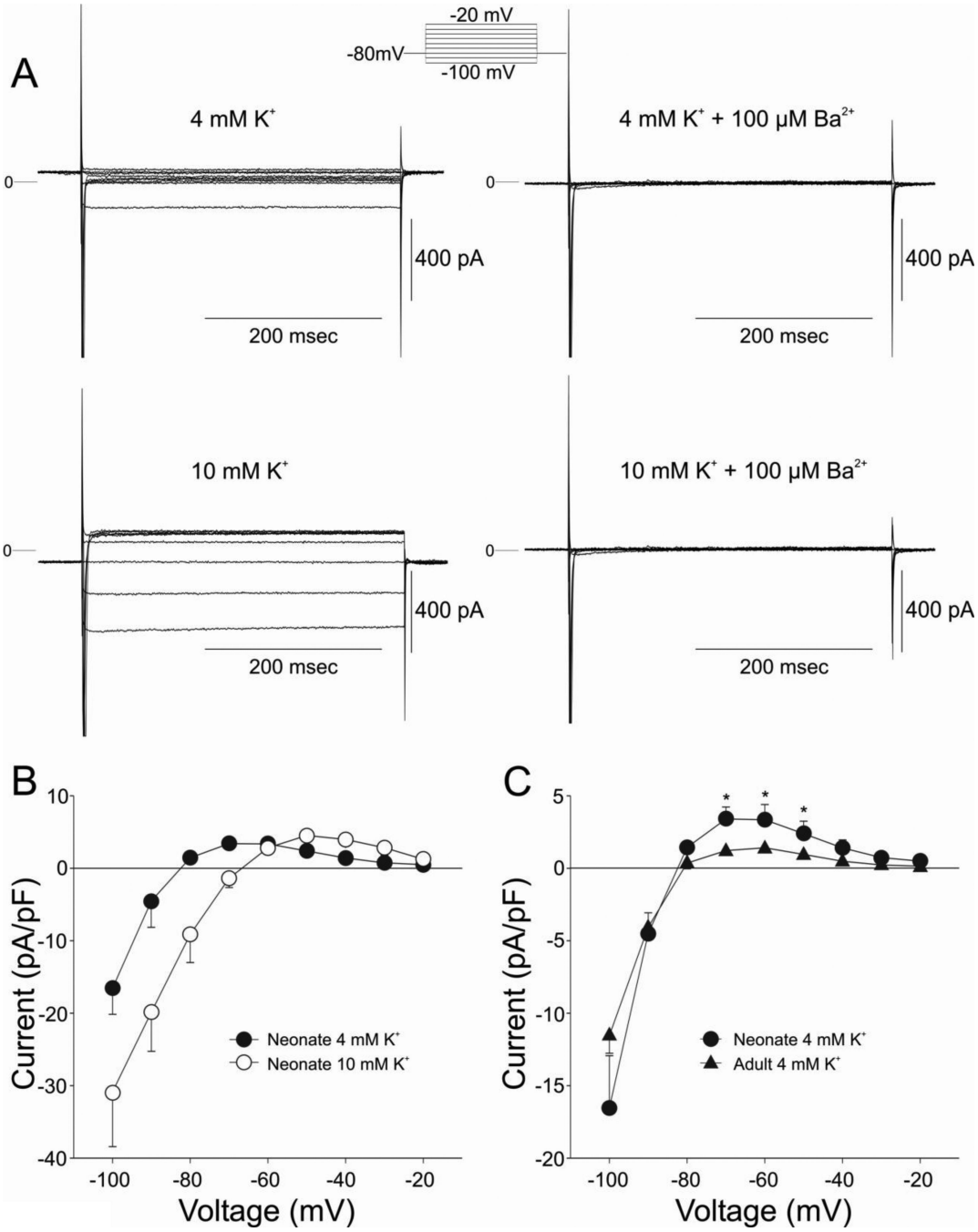

Figure 4.

Panel A: Representative currents recorded from a 2 week-old neonate ventricular myocyte in the absence and presence of 100 μM $BaCl_2$. Currents were elicited by stepping the voltage from the holding potential (−80 mV) to membrane potentials between −110 and −20 mV.**Panel B:** I-V relation for I_{K1} measured in normal conditions ($[K^+]_o$, 4.0 mM) as the Ba^{2+}-sensitive difference current. Raising $[K^+]_o$ to 10 mM resulted in an increase in I_{K1} and a crossing-over of the I-V relationships. **Panel C:** I_{K1} density in adult midmyocardial cells was less than that seen in neonate ventricular cells.

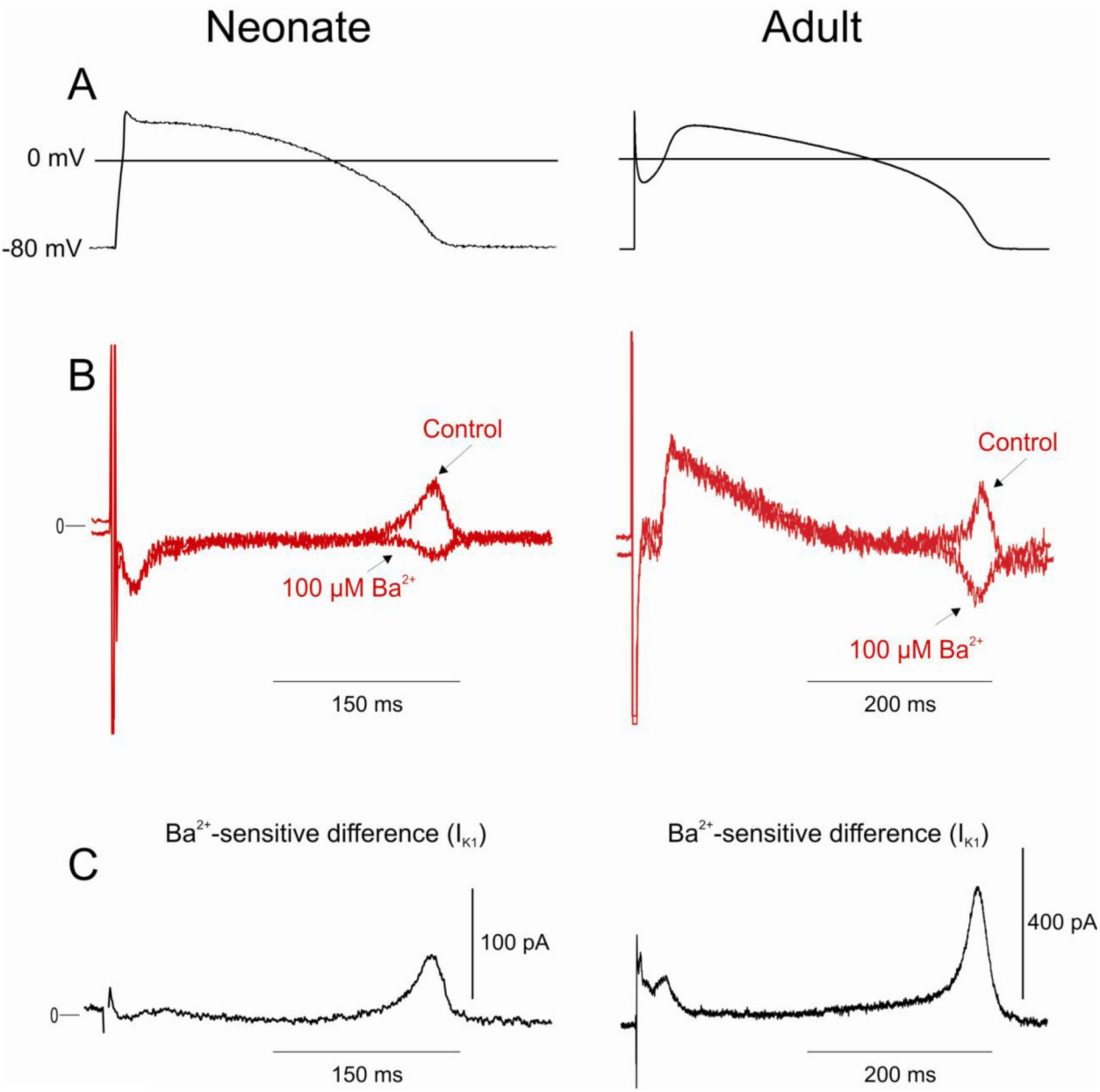

Figure 5.

Contribution of I_{K1} to ventricular repolarization in a 2 week-old neonate and adult mid cell assessed using an action potential voltage clamp. **Panel A:** Previously recorded APs from neonate or adult mid cells served as the waveform and the holding potential was −80 mV. **Panel B:** Superimposed current traces recorded during a train of 5 pulses in the absence and presence of 100 μM Ba^{2+}. **Panel C:** Subtraction of the 2 traces in **Panel B** yielded the Ba^{2+}-sensitive difference current.

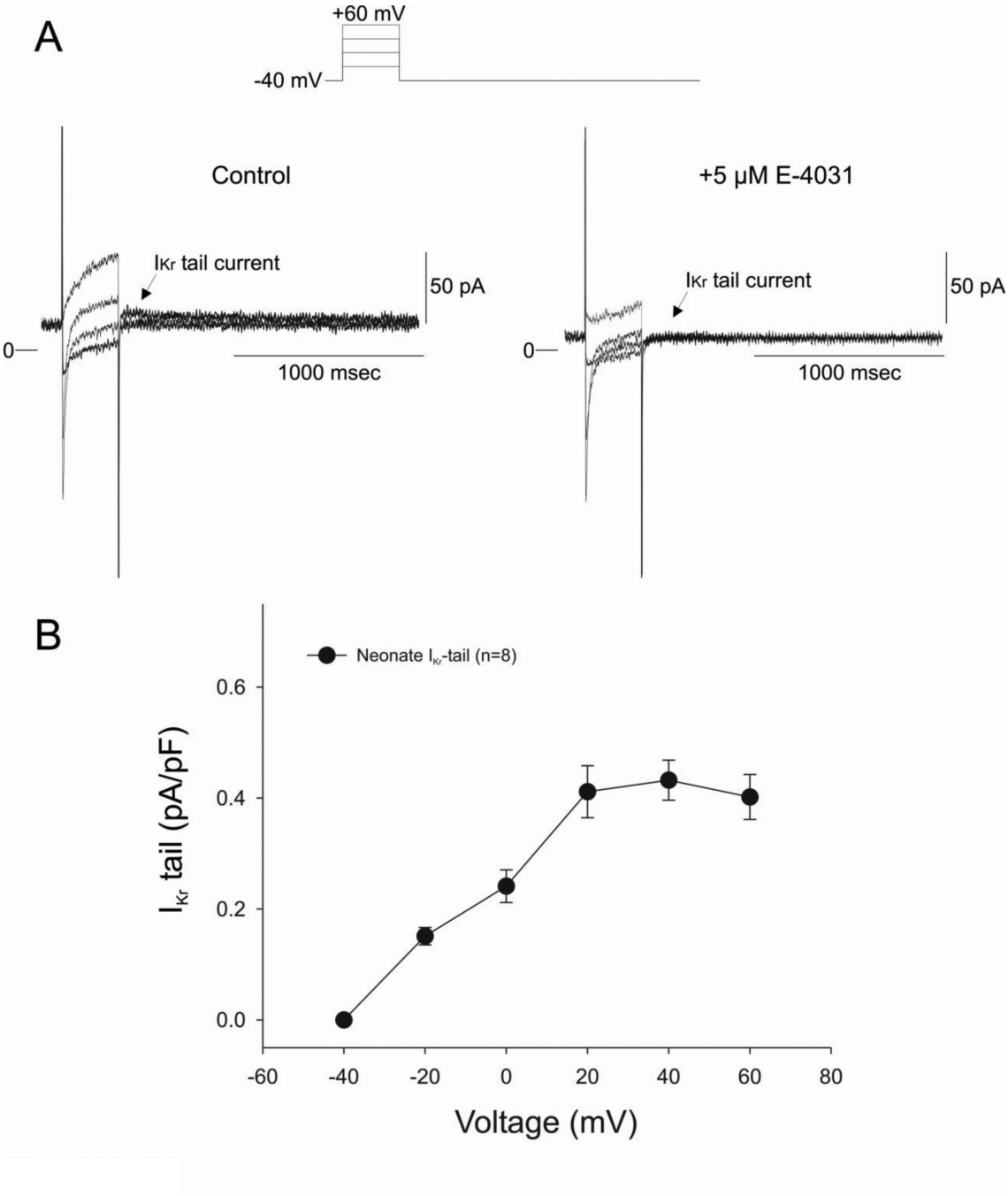

Figure 6.

Panel A: Representative current traces recorded from a 2 week-old neonate ventricular myocyte in the absence and presence of 5 μM E-4031. Application of 5 μM E-4031, an inhibitor of I_{Kr}, abolished the tail current. **Panel B:** Mean I-V relation for I_{Kr} tail current in neonate ventricular myocytes.

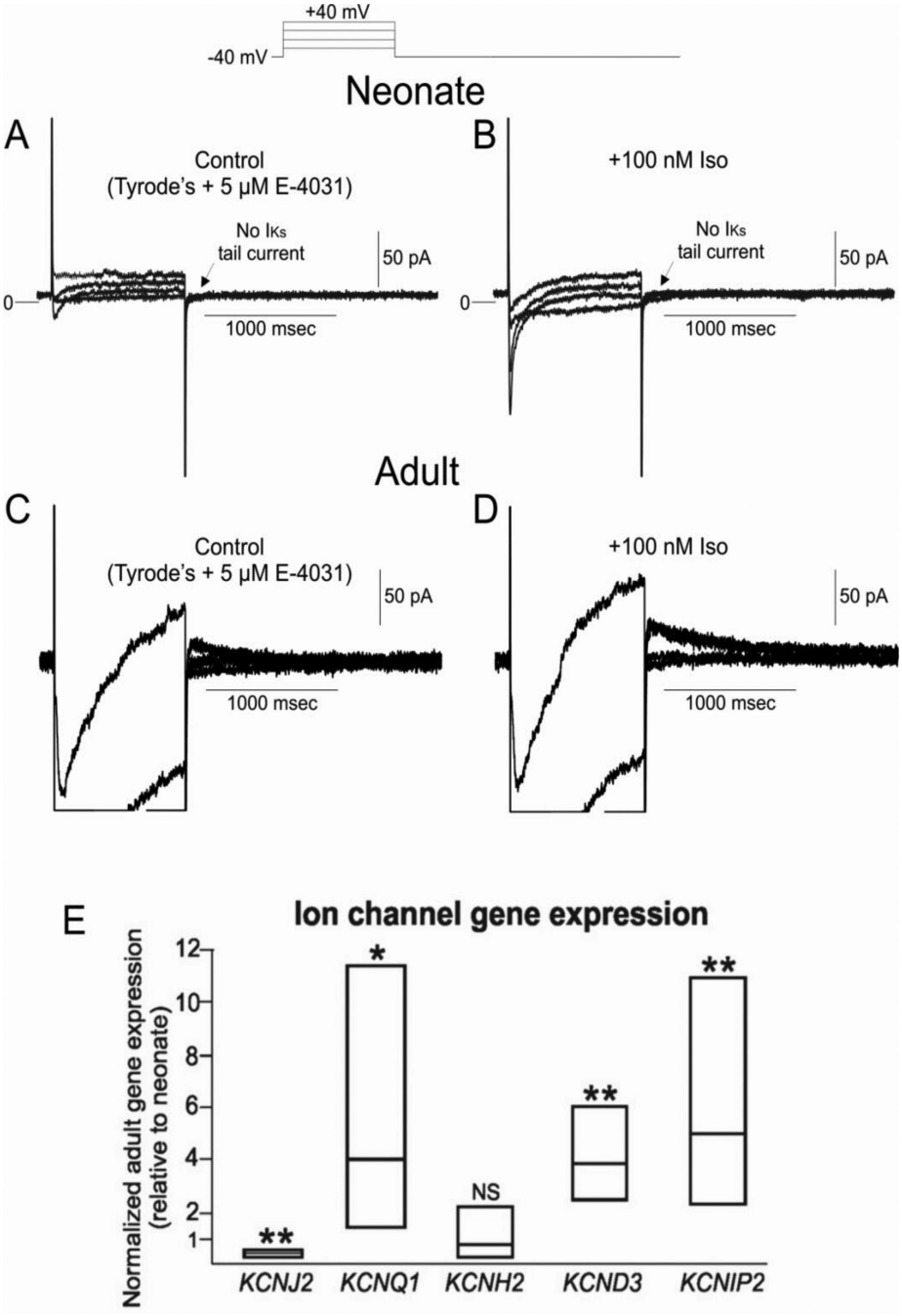

Figure 7.

Panel A: Representative I_{Ks} currents from 2 week-old neonate ventricular myocyte. E-4031 (5 μM) was present to eliminate I_{Kr}. I_{Ks} tail currents were not observed at any potential studied. **Panel B:** Protocol repeated in the presence of 100 nM isoproterenol. $_{ICa}$ was greatly augmented, although I_{Ks} was still absent. **Panel C:** Representative I_{Ks} currents from an adult ventricular myocyte. E-4031 (5 μM) was present to eliminate I_{Kr}. I_{Ks} tail currents were readily observed in adults using the same protocol. **Panel D:** I_{Ks} was augmented in the presence of 100 nM isoproterenol. **Panel E:** Ion channel gene expression in adult ventricular tissue (relative to neonatal). Data are presented as box plots with the mean together with upper and lower confidence levels (95%). *KCNQ1, KCND3* and *KCNIP2* are higher in adult

compared with neonate, while *KCNH2* is unchanged. *KCNJ2* is less in the adult ventricle compared with neonate.

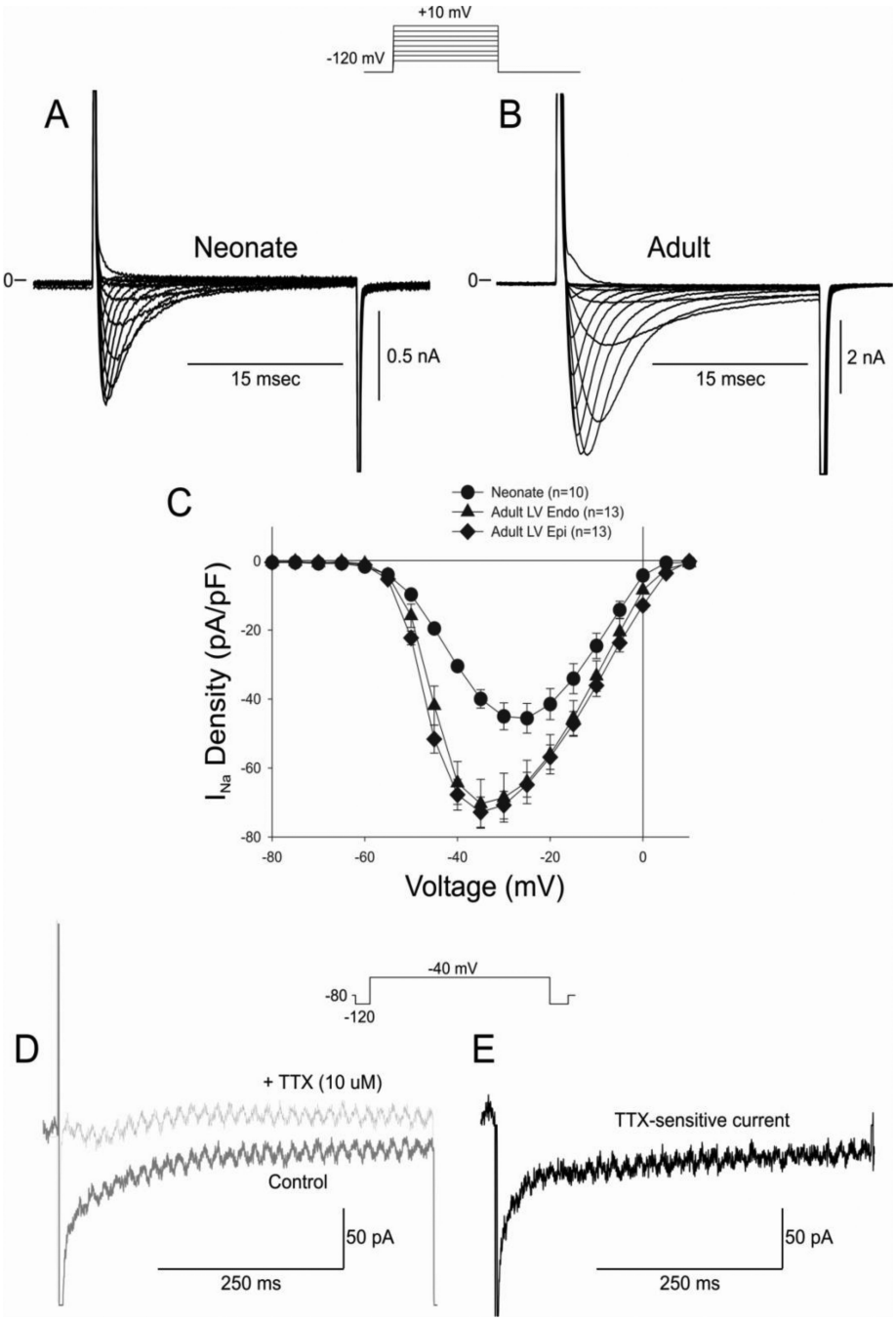

Figure 8.

Representative whole cell I_{Na} recordings from a 2 week neonate ventricular myocyte (**Panel A**) and adult ventricular myocyte (**Panel B**). Current recordings were obtained at test potentials between −80 and 10 mV in 5 mV increments from a holding potential of −120 mV. **Panel C:** I-V relation for 2 week neonate showing a significantly smaller I_{Na} compared to adult LV Epi or Endo. **Panel D:** Representative late I_{Na} recorded during a train of 5 pulses in control solution and after application of TTX (10 μM). **Panel E:** Subtraction of the traces shown in Panel D yielded the TTX-sensitive late I_{Na}.

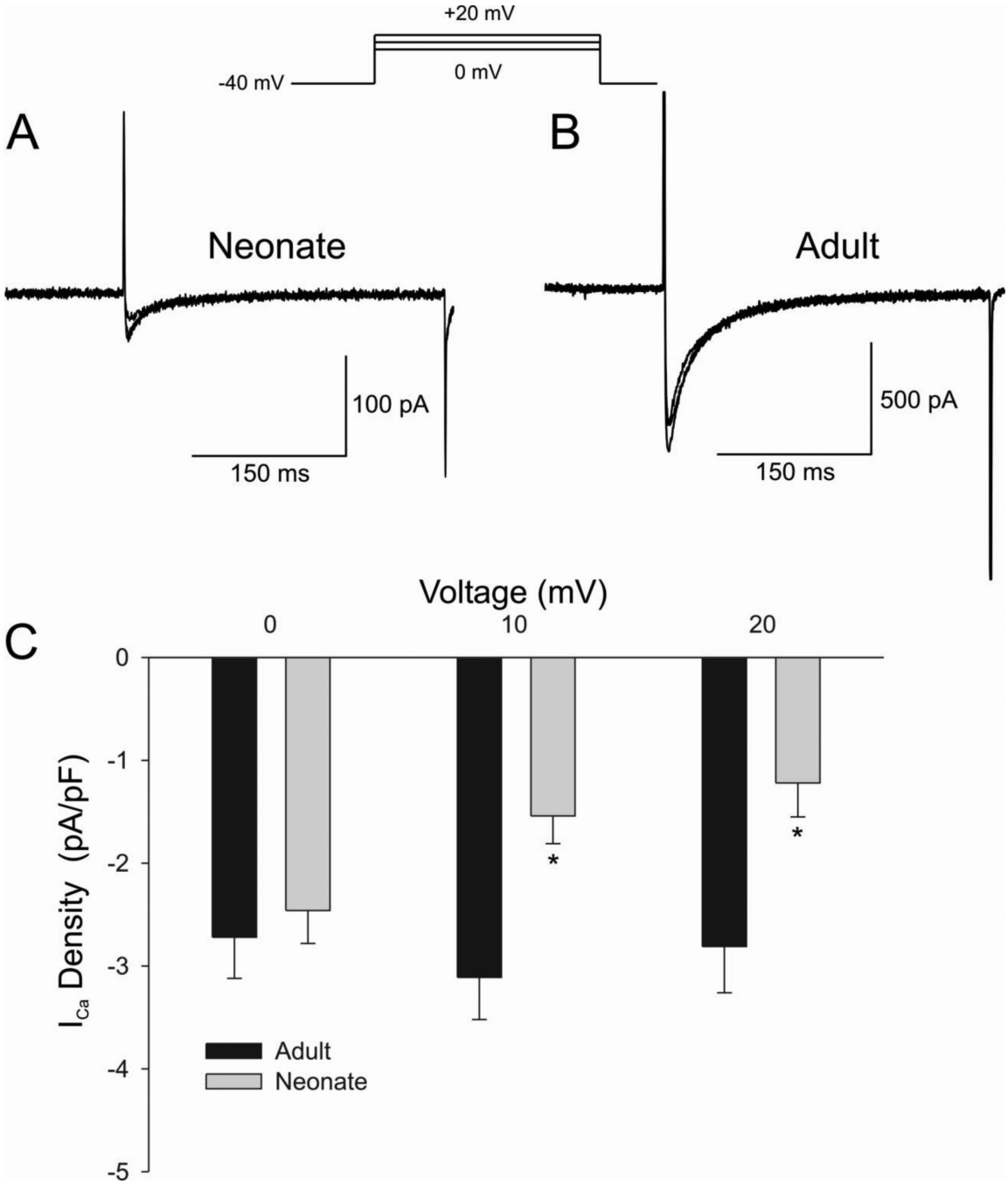

Figure 9.

Representative whole cell I_{Ca} recordings from a 2 week neonate ventricular myocyte (**Panel A**) and adult ventricular myocyte (**Panel B**). Current recordings were obtained at test potentials of 0, 10 and 20 mV from a holding potential of −40 mV. **Panel C:** Bar graph showing a significantly smaller I_{Ca} compared to adult midmyocardial cells.

Table 1

Effects of I_{Ks} and I_{Kr} Inhibitors on Tissue Layers from 2-week Neonates

	Control (APD_{90})	Chromanol (APD_{90})	% Increase	Incidence of EAD
Epi-	182±13 (n=5)	206±12 (n=5)	15±8	0/5
Mid-	203±13 (n=4)	208±8 (n=4)	4±3	0/4
Endo-	207±8 (n=4)	233±25 (n=4)	12±8	0/4

	Control (APD_{90})	Sotalol (APD_{90})	% Increase	Incidence of EAD
Epi-	190±10 (n=4)	274±27 (n=4)*	45±7*	0/4
Mid-	208±8 (n=5)	297±22 (n=5)*	43±6*	0/5
Endo	232±8 (n=4)	356±20 (n=4)*	53±7*	0/4

* significantly different from control at $p<0.05$